Immuno-suppressive Effect of Blocking the CD28 Signaling Pathway in T-cells by an Active Component of *Echinacea* Found by a Novel Pharmaceutical Screening Method

Guo-Chung Dong,[†] Ping-Hsien Chuang,[†] Michael D. Forrest,[‡] Yi-Chen Lin, and Hueih Min Chen*

Institute of BioAgricultural Sciences, Academia Sinica, Taipei, Taiwan 115, Republic of China

Received September 13, 2005

AFTIR (after flowing through immobilized receptor) is a novel method for screening herbal extracts for pharmaceutical properties. Using AFTIR, we identified Cynarin in *Echinacea purpurea* by its selective binding to chip immobilized CD28, a receptor of T-cells, which is instrumental to immune functioning. The results of surface plasma resonance show that binding between immobilized CD28 and Cynarin is stronger than the binding between CD28 and CD80, a co-stimulated receptor of antigen presenting cells. Cynarin's function was verified by its ability to downregulate CD28-dependent interleukin-2 (IL-2) expression in a T-cell culture line. AFTIR offers promise as an efficient screening method for herbal medicines.

Introduction

Herbal remedies, the use of plants to treat ill health, is the most ancient form of medicine.[1,2] It is common practice in the developing world while rapidly gaining popularity in the industrialized nations,[3,4] probably due to its reputedly low side effect and low cost. Its credibility, however, is hotly contested with detractors highlighting its principal foundation upon empirical observation as opposed to rigorous, randomized, double-blind, placebo-controlled trials. Despite this, there can be no doubt that it has given much to modern medical practice, with many of the pharmaceuticals currently available to western physicians having a long history as herbal remedies. Similarly, there is a wide-ranging consensus that it still has so much to offer, herbal remedies being sighted as untapped pharmaceutical repositories. Herbal medicines are complex mixtures containing up to thousands of compounds, only a minority of which are likely to have bioactivity. To realize herbal medicine's full potential, a high throughput drug screening initiative is required to isolate active ingredients from the 20,000 or so available herbal products. However, current screening methods for herbal compounds are heavily flawed, especially as they have no correlation to the concept of "targeting", which can be used to develop an efficient micro-array screening in the future. The traditional screening methods are composed of stages:[5,6] (1) solvent extraction; (2) high performance liquid chromatography (HPLC) or gas chromatography (GC) spectrum profiling; (3) major peak collection and identification by mass spectroscopy; (4) structural identification by nuclear magnetic resonance (NMR); and (5) bioactivity assay. This methodology assumes that an active ingredient will be an outstanding peak shown in the HPLC spectrum, which may not always be the case, and much inefficiency comes from the bioactivity not being assayed until so late in the sequence.

In this study, a novel screening method, after flowing through immobilized receptor (AFTIR;[a] Figure 1), is presented for targeting compound from herbal medicines. Basically it consists of a physiologically important receptor species being immobilized on a chip. Herbal extract is then driven to flow over this chip. Any molecular species that bind the receptor will become ensnared on the chip, and nonspecific species that do not bind the receptor will be flushed out from the chip by late washes. Any remaining binding species, being able to specifically bind this receptor in vitro, can be hypothesized to specifically bind this receptor in vivo and act pharmaceutically. They can be isolated and identified by modern analytical techniques such as mass spectrometry and nuclear magnetic resonance. This methodology can be iterated for differing immobilized receptor species and differing herbal extracts. In the present study, we immobilized CD28 (imm-CD28) on a chip and passed *Echinacea purpurea* extract across it. CD28 is a T-cell transmembrane receptor important to this cell class's differentiation to an activated state integral to cellular immune

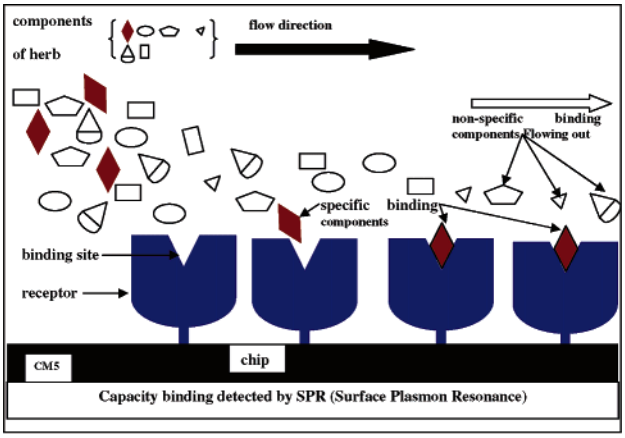

Figure 1. AFTIR concept. A receptor species is immobilized on a CM5 chip. Herbal extract, consisting of multiple component compounds (multiple symbols), is passed across the chip. Any molecular species that can specifically bind the receptor will become ensnared on the chip, from where it can be isolated (diamond symbol component specifically binds receptor). All other components flow across the chip without binding. Binding is detected by surface plasmon resonance (SPR).

* To whom correspondence should be addressed. Telephone: +886-2-2785-5696 ext. 8030. Fax: +886-2-2788-8401. E-mail: robell@gate.sinica.edu.tw or robell21@yahoo.com.

† First authorship for both.

‡ Current address: Department of Computer Science, University of Warwick, Coventry, CV4 7AL, UK.

[a] Abbreviations: AFTIR, after flowing through immobilized receptor; C1, compound 1; CEE, crude extract of *Echinacea*; IL-2, interleukin-2; imm-CD28, immobilized CD28; MTT, (3-[4,5-dimethylthiazol-2-yl]-2,5-diphenyltetrazolium bromide; PHA, phytohemaglutinin; PMA, phorbol 12-myristate 13-acetate; RU, response unit; SPR, surface plasma resonance; TSM, traditional screening method.

10.1021/jm0509039 CCC: $33.50
Published on Web 02/23/2006

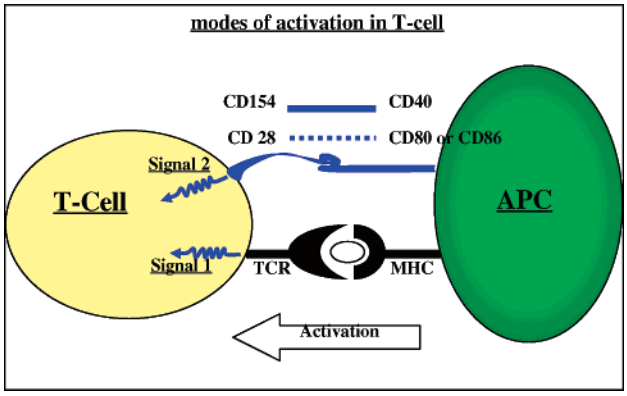

Figure 2. T-cell activation. T-cells differentiate to an activation state, a state instrumental to the immune response, in retort to co-stimulation by two antigen presenting cell (APC) signals. Signal 1: Major histocompatibility complex (MHC) of APC cell strongly binds T-cell receptor (TCR) of T-cells. Signal 2: CD80 or CD86 (both APC cell) weakly binds CD28 of T-cells, and CD40 of APC cell strongly binds CD154 of T-cell.

response, which is partly characterized by interleukin-2 (IL-2) secretion (see Figure 2; signal 2, co-stimulations of CD28 and CD154 with CD80 (or CD86) and CD40, respectively). *Echinacea purpurea* is a flower native to North America, first used medicinally by the Native Americans and now popular in Europe and America for its purported, yet heavily debated, boosting of the immune system.[7−10] Using AFTIR methodology, an *Echinacea* constituent compound was found that could selectively bind CD28. This compound was expected to have an immunosuppressive action in the body, perturbing physiological functioning of CD28. The presented in vitro studies support this hypothesis, with this compound found to downregulate CD28-dependent IL-2 expression in Jurkat cells, a T-cell culture line.[11] Mass spectrometry and NMR spectroscopy identified this compound as Cynarin, which has been well studied, but its immuno-suppressive function is a novel finding. *Echinacea purpurea* also acts immuno-suppressantly in this assay, constituent Cynarin being the likely active compound. This finding is contrary to *Echinacea*'s purported boosting of the immune system and may need to be taken into consideration given its popular use in the treatment of upper respiratory disorders, minor infections, herpes, candida, eczema, and AIDS-related opportunistic infections.

Results

Immobilization of CD28 Receptor on the Chip. CD28-muIg, a soluble fusion protein consisting of the extracellular (134 aa) domain of human CD28 fused to murine IgG2a Fc (233 aa), was immobilized to dextran matrix on the sensor chip surface, via covalent coupling of primary amines ($-NH_2$). In this report, the term CD28 will be used as shorthand for CD28-muIg. The strength of binding was assayed by the response unit (RU), using surface plasma resonance (SPR; see Materials and Methods). Figure 3a shows the corresponding sensorgram. The "binding capacity", ΔR ($\Delta R \simeq R'' - R'$; see Figure 3a), of CD28 on the sensor chip was approximately 15 ng/mm^2 surface coverage (15,000 response units (RU); 1 RU = 1 pg/mm^2). Although CD28 was fully immobilized on the chip, it retained its native binding activity because it was found to bind strongly and specifically to CD28 antibody (or anti-CD28; see Figure 3b (test 1), where $\Delta R = \sim 310$ RU with 10 μg/mL anti-CD28) and to bind relatively weakly to CD80 (see Figure 3c (test 2), where $\Delta R = \sim 120$ RU with 10 μg/mL CD80). The results of test 1/test 2 above and the co-stimulation of weak binding between CD28 and CD80 can be referred to in Figure 2, signal 2.

AFTIR methodology relies not simply on selective molecular binding to the chip, but also on the ability to dissociate bound molecules for identification and reuse of the chip. Various washing solutions were tested, with 50 mM NaOH performing the best. Figure 3d (test 3) shows a typical sensorgram for anti-CD28 binding ($\Delta R = R'' - R' \approx 600$ RU with 10 μg/mL anti-CD28) followed by interactions with NaOH washing solution (concentration = 50 mM; flux = 50 μL/min; time = 10 s). After washing, the anti-CD28 was largely dissociated, with the binding affinity almost equal to the pre-antibody application value ($R' = \sim R'''$). One hundred cycles of this same anti-CD28 application and washing protocol were performed on the same chip. Figure 3e (test 4) plots R''' as a percentage of R', against iteration number, for 25 of these 100 iterations; R''' was never less than 95.4% of R' in this iteration range. Figure 3f (test 5) shows the anti-CD28 binding capacity ($\Delta R = R'' - R'$, see Figure 3d) against iteration number. For 100 cycles, mean ΔR = 598 RU, with a relative standard deviation (RSD) of 2.43%. Based on the results of tests 1−5, the chip is reusable and the experimental setup is reliable.

Crude Extract of *Echinacea* (CEE) Binds CD28 Immobilized on the Chip. Figure 4 shows a typical sensorgram for crude extract of *Echinacea* (CEE) binding to CD28 immobilized on the chip ($R' = \sim 851$ RU). Most extract material was bound nonspecifically and subsequently dissociated. The remaining extract material bound specifically to CD28 ($\Delta R \simeq R'' - R' = \sim 70$ RU) and was only removed by the washing protocol (described previously). The sharp changes of RU observed at time points of R' and R'' across the time course indicate the high affinity binding of CEE to the chip.

CEE Can Block CD80 Binding CD28 Immobilized on the Chip. To look at the competition among the bindings between receptor and CEE (or CD80) or between receptor and antibody, the following time series was conducted: CD80 (10 μg/mL; 30 μL) was fluxed across CD28 immobilized on the chip (see Figure 5a, step 1). The binding capacity (before the dissociation) of CD80 associated with imm-CD28 is indicated by ΔR_0. After washing (Figure 5a, step 2), CEE was fluxed across the same chip (Figure 5a, step 3). CD80 (10 μg/mL; 30 μL) was then again fluxed across the CD28 immobilized on the chip (Figure 5a, step 4). The binding capacity of CD80 with imm-CD28 is indicated by ΔR_1. The results show $\Delta R_0 > \Delta R_1$, which indicates that CD80 did not bind as well. This time series was repeated with anti-CD28 in place of CEE, with an equivalent result ($\Delta R_0 > \Delta R_1$; data not shown). Therefore, CEE and anti-CD28 evidently (at least partially) blocked CD80 binding.

Figure 5b shows the binding of differing concentrations (0, 5, 10, 25, 50, and 100 μg/mL of CD80 to immobilized CD28. Figure 5c shows the binding of differing concentrations (0, 5, 10, 25, 50, and 100 μg/mL) of CD80 to immobilized CD28, which was previously fluxed with anti-CD28. Figure 5d shows the binding of differing concentrations (0, 5, 10, 25, and 50 μg/mL) of CD80 to immobilized CD28, which was previously fluxed with CEE. Figure 5b−d is baselined with the subtraction of "background RU", the RU present in the absence of immobilized CD28. Plots in Figure 5b−d exhibit plateauing (saturation of binding), from which, using the standard Langmuir binding isotherm, the values of k_a (association constant; M^{-1}) and k_d (dissociation constant; s^{-1}) were calculated. Affinity binding constants ($1/K_D$) were then obtained from the K_D's, where K_D's were calculated from Scatchard plots and presented

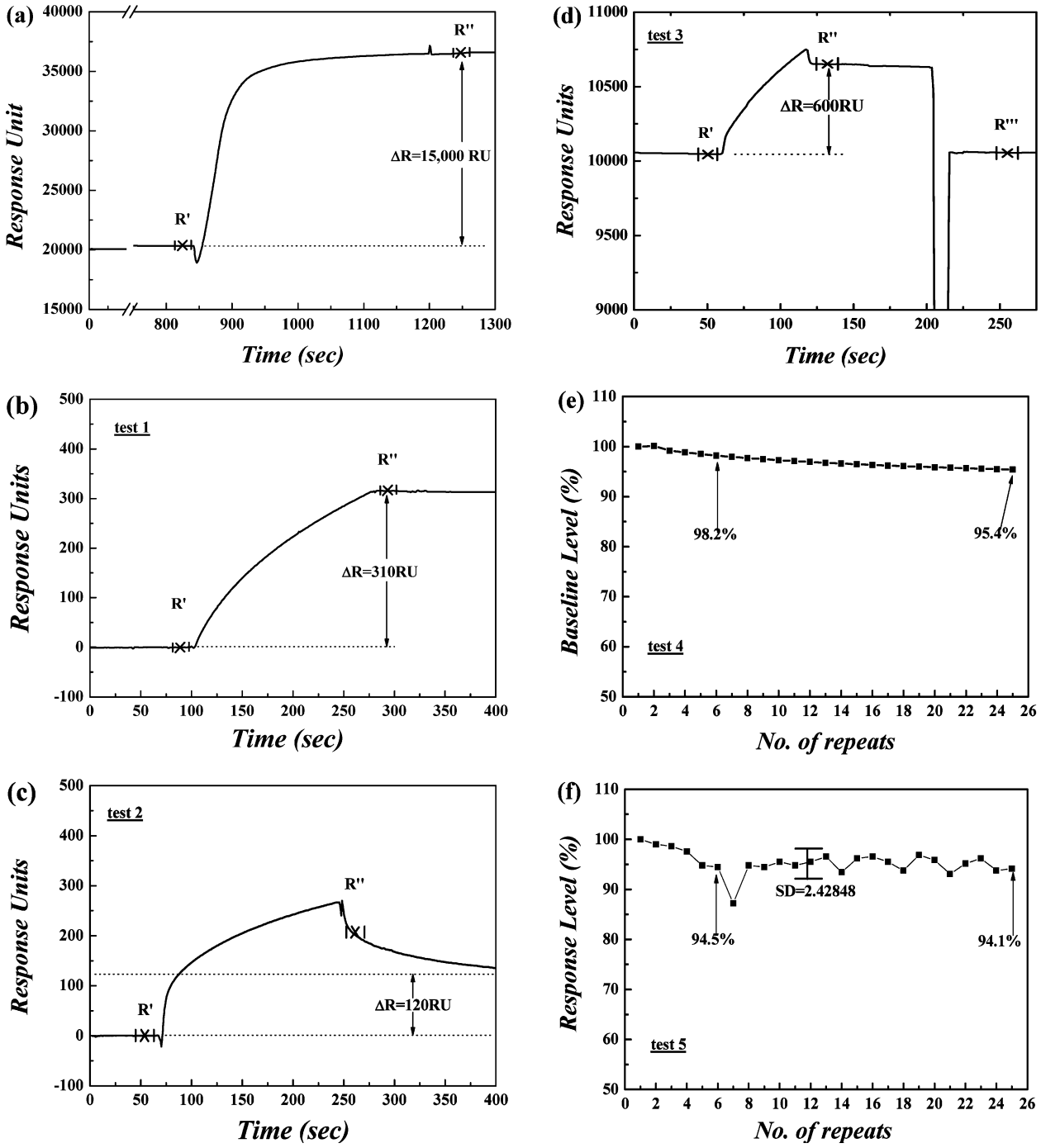

Figure 3. Immobilization of CD28 receptor on the chip. (a) Sensorgram of CD28 binding chip. CD28 binds strongly with a "binding capacity", ΔR ($\Delta R = R'' - R'$), of ~15,000 RU. (b) Anti-CD28 strongly binds imm-CD28. ΔR = ~310 RU. (c) CD80 weakly binds imm-CD28. ΔR = ~120 RU. (d) Typical sensorgram for anti-CD28 binding (ΔR = ~600 RU with 10 μg/mL anti-CD28) and subsequent NaOH washing (concentration = 50 mM; flux = 50 μL/min; time = 10 s). After washing, anti-CD28 was largely dissociated, with a binding affinity almost equal to the pre-antibody application value ($R' = \sim R''$). (e) R'' as a percentage of R (as shown in Figure 3d) for 25 [anti-CD28 binding and then NaOH washing] cycles. R''' was never less than 95.4% of R'. (f) Anti-CD28 binding capacity ($\Delta R \simeq R'' - R'$, as shown in Figure 3d) for 25 [anti-CD28 binding and then NaOH washing] cycles. Relative standard deviation (RSD) = ~2.4%.

in Table 1. CD80 bound immobilized CD28 at $1/K_D = 9.1 \times 10^5$ M^{-1}. This CD80−CD28 binding is weaker in the presence of anti-CD28 ($1/K_D = 8.5 \times 10^4$ M^{-1}) and CEE ($1/K_D = 4.9 \times 10^5$ M^{-1}). Quantitatively reiterating what was shown previously, CEE and anti-CD28 evidently (at least partially) block CD80 binding.

After C1 compound was identified as a Cynarin (see Chemical Identification of C1), the binding experiments between Cynarin−CD28 and CD80−CD28 were conducted again by AFTIR. Both the equilibrium constant (K_d ($=k_d/k_a$)) and the dissociation rate constant (k_d) were 1.7×10^{-7} M and 2.94×10^{-5} s^{-1}, respectively, for Cynarin−CD28 and 1.11×10^{-6} M and 1.04×10^{-2} s^{-1}, respectively, for CD80−CD28. The results indicated that Cynarin had higher affinity to CD28 than did CD80. The lower k_d of Cynarin−CD28 implied the capable binding of Cynarin to CD28. Furthermore, in AFTIR experiment, one observed that only target compound(s) were able to bind to the receptor immobilized on the chip.

HPLC Profiling of CEE. We had shown that CEE component(s) were able to selectively bind CD28, but what were these

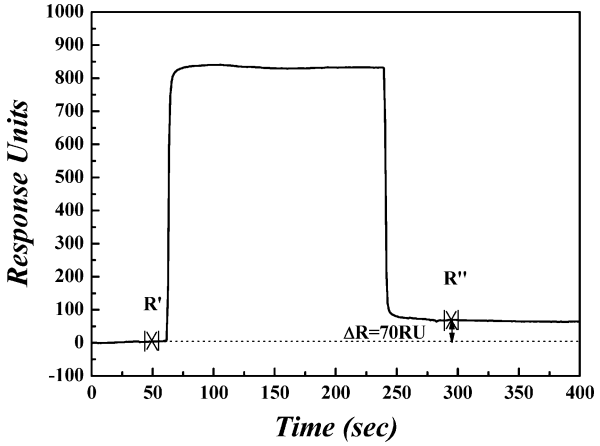

Figure 4. Crude extract of *Echinacea* (CEE) binds chip immobilized-CD28. A typical sensorgram for CEE binding CD28 immobilized on a chip ($R' = \sim$851 RU). Most extract material is bound nonspecifically and subsequently dissociates. The remaining CEE material is bound specifically to CD28 ($\Delta R \simeq R'' - R' = \sim$70 RU). It can be removed by the NaOH washing protocol. The sharp changes at times R' and R'' across the time course indicate high affinity binding of CEE to the chip.

components? Bound CEE was washed off the chip and profiled with HPLC (Figure 6C−G); six reproducible results from independent experiments). There are three discernible peaks (demarked 1, 2, and 3), indicating three CEE compounds (C1, C2, and C3, respectively) bound CD28, and establishing that these compounds bound the CD28 immobilized on the chip, but not the chip itself. CEE "wash off" from a chip with no immobilized receptor was profiled (Figure 6B); as can be seen, no peaks were visible, indicating the specificity of CEE components binding to CD28. In contrast, Figure 6A shows the added complexity of spectrum obtained with CEE in the absence of AFTIR processing. In addition to the three peaks 1, 2, and 3 (see AFTIR 6C−G), more peaks existed. Figure 7A shows this spectrum again, with Figure 7B−E showing the spectrums of isolated compounds C4, C1, C3, and C5, respectively (where C4 and C5 were for references). C2 could not be isolated due to its small quantity. C1 and C3, being able to bind CD28 based on our AFTIR results, were hypothesized to have CD28 bioactivity, while C4 and C5 were not.

Table 1. Kinetic Values for CD80 Binding Chip Immobilized CD28, with or without Prior Anti-CD28 or Crude Extract of *Echinacea* (CEE) Binding to Immobilized CD28

binding conditions	parameters		
	k_a (M^{-1})	k_d (s^{-1})	$1/K_D$ (M^{-1})
imm-CD28 → CD80	12.4×10^3	10.4×10^{-3}	9.1×10^5
imm-CD28 → (anti-CD28) → CD80	2.9×10^3	5.7×10^{-3}	8.5×10^4
imm-CD28 → (CEE) → CD80	8.6×10^3	4.2×10^{-3}	4.9×10^5

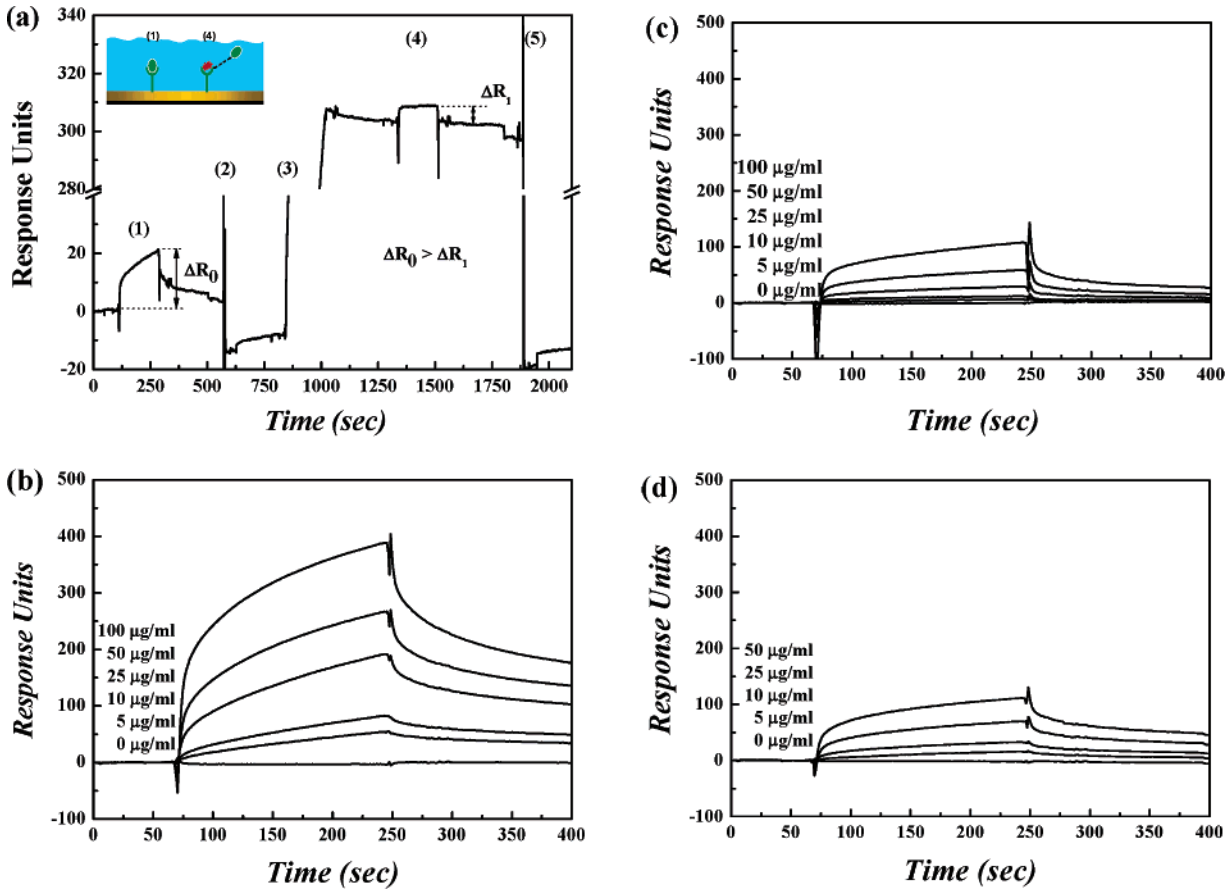

Figure 5. Crude extract of *Echinacea* (CEE) blocks CD80 binding to chip immobilized-CD28. (a) Sensorgram. CD80 binds chip immobilized CD28 (step 1; binding capacity = ΔR_0). NaOH washing removes bound CD80 (step 2). CEE binds chip immobilized CD28 (step 3). CD80 presented to chip immobilized CD28 (step 4; binding capacity = ΔR_1). CEE bound partially blocks CD80 binding because CD80 does not bind as well as previously ($\Delta R_0 > \Delta R_1$). The inset figure (left) shows CD80 (circle) bound to chip immobilized CD28 (Y-shape) in step 1 and (right) CEE (star) binding CD28, thus blocking CD80 binding in step 4. (b) The binding of differing CD80 concentrations (0, 5, 10, 25, 50, and 100 μg/mL, bottom to top) to immobilized CD28. (c) The binding of differing CD80 concentrations (0−100 μg/mL) to immobilized CD28, previously fluxed with anti-CD28 (10 μg/mL). (d) The binding of differing concentrations of CD80 (0−50 μg/mL) to immobilized CD28, previously fluxed with CEE (10 μg/mL). Parts b−d are base-lined with the subtraction of "background RU", where RU represents the chip without immobilized CD28.

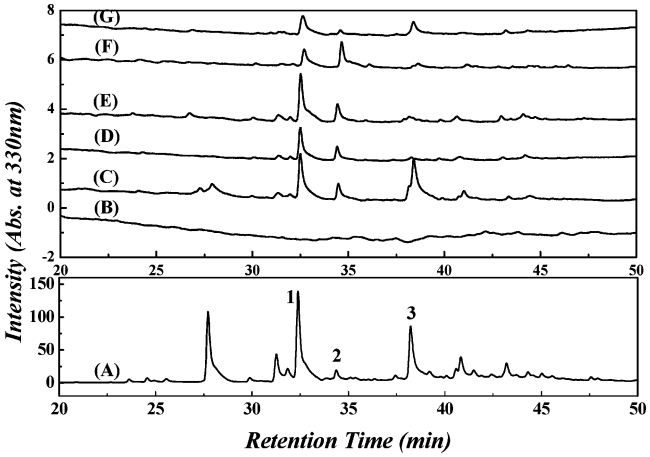

Figure 6. HPLC profiling of crude extract of *Echinacea* (CEE). (A) HPLC profile (absorption at $OD_{330\,nm}$ vs retention time) of CEE untreated by AFTIR. Discernible peaks 1, 2, and 3. (B) HPLC profile of the CEE fraction passed over the chip with no immobilized CD28 (control). (C−G) HPLC profiles of the CEE fraction expected to chip immobilized CD28. There are three discernible peaks corresponding to the peaks shown in (A) demarked by 1, 2, and 3.

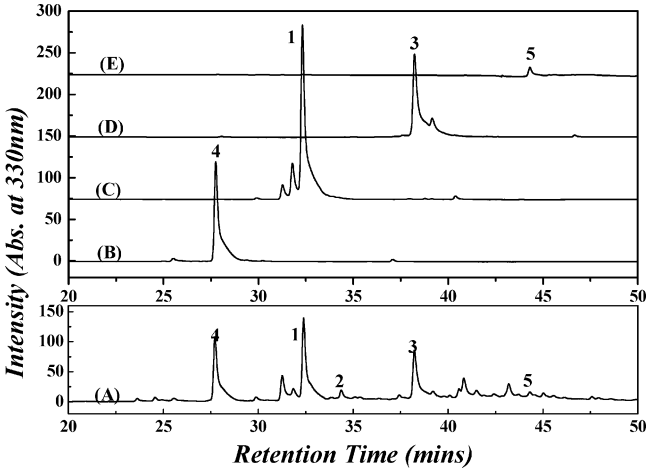

Figure 7. Compound isolation with HPLC profiling. (A) HPLC spectrum of CEE. Peaks 1−5 denote compounds C1−C5. (B−E) are the HPLC spectrums of isolated compounds C4, C1, C3, and C5, respectively.

Bioassay of Compounds Highlighted by AFTIR. We had thus far established those components of CEE extract could selectively bind CD28. CD28 is a T-cell transmembrane receptor, integral to this cell class's differentiation to its "active" state, a state that can be characterized by interleukin-2 (IL-2) secretion. We now determine whether either of these CEE components could downregulate IL-2 secretion in Jurkat cells by binding to CD28 receptor on the cell surface.

Jurkat cells can differentiate to the "active state" in response to one of two activating signals: (1) phorbol 12-myristate 13-acetate (PMA) and ionomycin (CD28-independent pathway)[12−17] and (2) anti-CD3 and anti-CD28 (CD28-dependent pathway)[18−22] (Figure 8 shows the pathways in detail). The Jurkat cells without activators above produced little IL-2 (Figure 9, blank). IL-2 secretion significantly increased upon application of PMA and ionomycin or anti-CD3 and anti-CD28 (see Figure 9, −cont. 1200 pg/mL of IL-2 released was normalized to 100%). This significant secretion with either of the activating signals was eradicated by the additional application of FK506, a clinical immunosuppressant (Figure 9, +cont.). CEE application was found not to modulate the IL-2 secretion response of Jurkat cells to PMA and ionomycin but did significantly downregulate

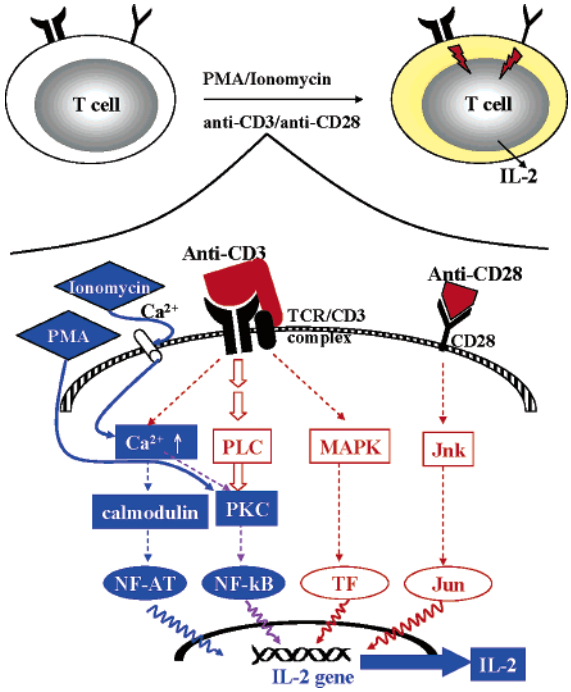

Figure 8. Jurkat cell activation. Jurkat cells can differentiate to the activated state, characterized by interleukin-2 (IL-2) secretion, in response to one of two activatory signaling profiles: (1) Phorbol 12-myristate 13-acetate (PMA) and ionomycin (CD28-independent pathway) and (2) anti-CD3 and anti-CD28 (CD28-dependent pathway). The associated cascades: PMA→PKC→NF-kB; ionomycin→Ca^{2+}→calmodulin→NF-AT; anti-CD28→CD28→Juk→Jun. Anti-CD3 works through three pathways: (i) anti-CD3→CD3/TCR→MAPK→TF; (ii) anti-CD3→CD3/TCR→PLC→PKC→NF-kB; (iii) anti-CD3→CD3/TCR→Ca^{2+}→calmodulin→NF-AT. Target transcription factors (NF-AT, NF-kB, TF, Jun) upregulate IL-2 expression.

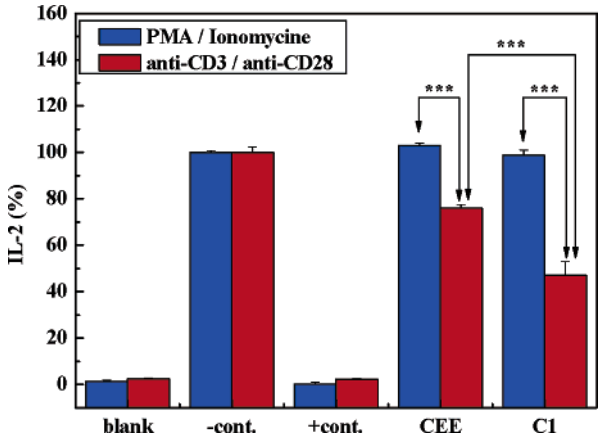

Figure 9. In vitro immuno-suppressive action of CEE and C1. Jurkat cells (5×10^5 cells/mL), treated with PBS buffer, produce little IL-2 (blank). IL-2 secretion significantly increases with application of PMA and ionomycin or anti-CD3 and anti-CD28 (these stimulations were used as reference for negative controls (−cont.); 1200 pg/mL of IL-2 released from these stimulations was normalized to 100%). These significant secretions with either of the activation molecules above were inhibited by the additional application of FK506 (1 μg/mL), a clinical immuno-suppressant (the results of FK506 were used as positive controls (+cont.). CEE or C1 (both 100 μg/mL) application does not modulate an IL-2 response to PMA and ionomycin, but significantly downregulates (−22%, −53%, respectively) IL-2 production in response to anti-CD3 and anti-CD28 (CEE, C1).

(−22%) the IL-2 secretion response to anti-CD3 and anti-CD28 (Figure 9, CEE). CEE therefore did disrupt CD28-dependent signaling in this in vitro experiment. None of compounds C2−

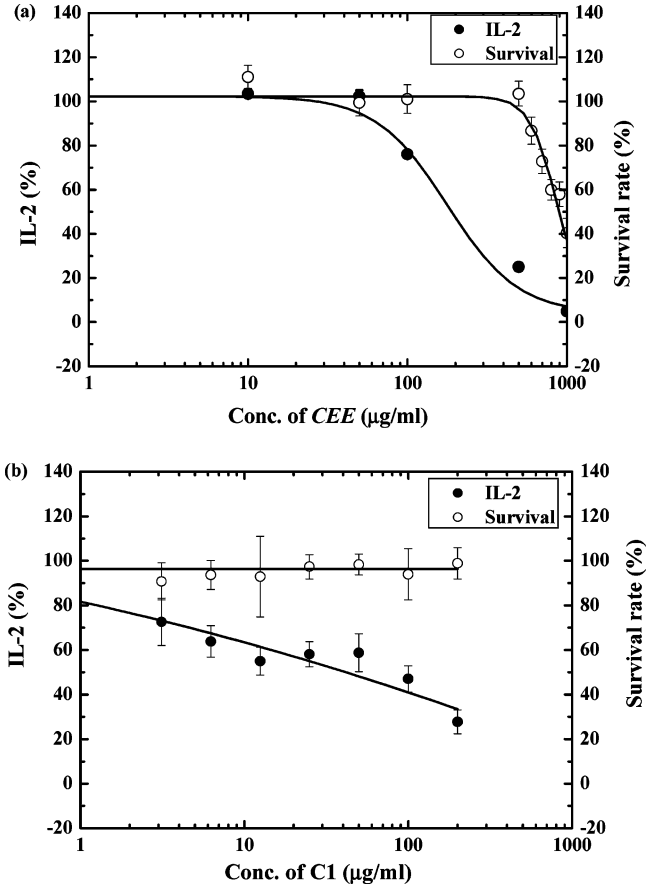

Figure 10. IL-2 and cytotoxicity in response to the concentration of CEE and C1. (a) IL-2 response to anti-CD3 and anti-CD28 (%, ●), and cell survival (%, ○), in relation to the concentration of CEE (μg/mL) applied. CEE only inhibits IL-2 response at concentrations >10 μg/mL and is not toxic at concentrations <500 μg/mL. Part (b) is as (a), but substitutes C1 for CEE. C1 linearly reduces IL-2 response, with no toxicity, across the concentration range investigated.

C5 can modulate IL-2 response to either of the activating signals (data not shown). C1, however, although unable to modulate any response to PMA and ionomycin, significantly downregulated (−53%) response to anti-CD3 and anti-CD28 more than CEE (Figure 9, C1). Figure 10a shows (1) Jurkat IL-2 response to anti-CD3 and anti-CD28 (●) and (2) Jurkat cell survival (%, ○), in relation to the concentration of CEE applied. Figure 10b shows the same dependent variables, but in relation to C1 concentration. CEE only inhibited IL-2 response at concentrations >10 μg/mL and was not toxic at concentrations <500 μg/mL. Addition of C1 to Jurkat cells was found to linearly reduce IL-2 response, with no toxicity, across the concentration range investigated.

Chemical Identification of C1. C1 was chemically identified by mass spectrometry and NMR spectroscopy (^{13}C and ^{1}H) as Cynarin[23−25] (1,3-dicaffeoylquinic acid) (its formula, see Figure 11). C1 exhibited an $[M + 1]^+$ peak at $m/z = 517$, indicating its molecular weight as that of Cynarin. Cynarin has a quinic acid moiety. ^{13}C NMR and DEPT experiments showed such a moiety in C1, with two methylenes (δ36.7, δ41.3), three oxymethines (δ68.3, δ73.0, δ74.8), one quaternary carbon (δ75.4), and one carboxyl group (δ178.3). ^{1}H NMR signals from protons at C-2′,2″, C-5′,5″, C-6′,6″, C-7′,7″, and C-8′,8″, in the 6−8 ppm region, were closely approximated to those of the two caffeoyl moieties in Cynarin (very slight shift). The ^{13}C NMR data of C1 also indicated the existence of the two caffeoyl moieties on the related chemical shift values.

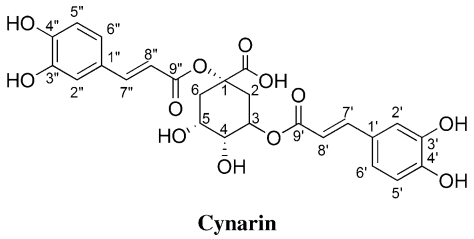

Cynarin

Figure 11. Structure of C1. Mass spectrometry and NMR spectroscopy identify C1 as Cynarin (1,3-dicaffeoylquinic acid).

Comparisons of the chemical shifts of ^{1}H NMR and ^{13}C NMR for C1 and Cynarin identified previously[23,24] were shown in Table 2. The results imply that C1 is a Cynarin.

Discussion

AFTIR (after flowing through immobilized receptor) is a novel method of screening herbal extracts for potential pharmaceuticals. In this study, it was employed to screen *Echinacea* for the potential constituent immuno-suppressant to CD28, a receptor of T-cell instrumental to immune functioning. Crucially, binding of CD28 to the chip in AFTIR was shown to be strong and also nonimpairing to its native binding activity because chip-bound CD28 could still bind both antibody and CD80. Furthermore, these binding species could be dissociated by NaOH, rendering the chip reusable, given that chip-bound CD28 was shown to have maintained binding affinity after repeated binding−dissociation cycles. Using this chip, an *Echinacea* component was shown to selectively bind CD28, partially blocking subsequent anti-CD28 and CD80 binding. HPLC profiling showed this component to consist of three compounds, one of which, identified by mass spectrometry and NMR spectroscopy as Cynarin, was shown in this study to be an immuno-suppressant in vitro, downregulating CD28-dependent IL-2 expression in Jurkat cells (at nontoxic concentrations). Our hypothesis for Cynarin's mechanism of action is that it binds to the extra-cellular part of CD28, disrupting CD28−CD80 binding and thus disturbing CD28-dependent T-cell activation. It could perhaps prove medicinal in autoimmune or organ transplant cases. Furthermore, crude extract of *Echinacea purpurea* was also shown to act immuno-suppressantly in vitro, constituent Cynarin being the likely main active compound. This is concerning given *Echinacea*'s wide pattern of use based on its upregulation of immune functioning. Such use might be moderately harmful. In clinical support for outpatients, *Echinacea* prescription has been weakly associated with adverse effects in pediatric patients.[7]

AFTIR is compared to the traditional screening method (TSM) in Figure 12. Both use HPLC to separate constituent extract compounds, such that they may be independently tested in bioassay(s), for example, the Jurkat IL-2 expression protocol in this report. However, AFTIR is more efficient as its partitioning step actually incorporates a bioassay, assessing whether any extract component can bind a rationally chosen receptor species. With AFTIR, only the extract component that can bind receptor is profiled with HPLC, yielding a spectrum much reduced in complexity, greatly simplifying the HPLC process. In addition, AFTIR does not hinge on the unreliable assumption, integral to TSM, that active ingredients are major peaks in the HPLC spectrum. However, the complexities of AFTIR are due to the "orientation" of receptors when immobilized on the chip and the "quantity" of bound molecules collected from the immobilized receptors.

In summary, this study shows how AFTIR could provide an efficient screening method for potential herbal immuno-related

Table 2. Comparisons of Chemical Shifts of ^{1}H NMR and ^{13}C NMR for C1 Compound and Cynarin[23,24]

^{1}H NMR (CD_3OD, 400 MHz)

	C1	Cynarin[a]	Cynarin[b]
C2,6-H	2.03−2.13 (2H, m), 2.16−2.28 (2H, m)	1.83−2.87 (4H, m)	2.24 (1H, dd, J = 15.6, 3.6 Hz), 2.67 (2H, m)
C3-H	3.85 (1H, m)	5.36 (1H, m)	4.23 (1H, m)
C4-H, C5-H	3.55 (1H, d, J = 4 Hz), 3.15 (1H, dd, J = 3, 9 Hz)	3.61 (1H, dd, J = 3.6, 9.6 Hz), 4.22 (1H, ddd, J = 4.4, 9.6, 11.2 Hz)	3.71 (1H, dd, J = 9.6, 3.2 Hz)
caff -OH	4.81 (4H, s)		5.43 (1H, m)
caff C8′,8″-H	6.18 (2H, d, J = 16 Hz)	6.11 and 6.18 (1H each, d, J = 15.9 Hz)	6.18 (1H, d, J = 16.0 Hz), 6.24 (1H, d, J = 16.0 Hz)
caff C5′,5″-H	6.74 (2H, d, J = 8 Hz)	6.50 and 6.63 (1H each, d, J = 8.2 Hz, H-5′, -5″)	6.76 (2H, d, J = 8.0 Hz)
caff C6′,6″-H	6.89 (2H, dd, J = 2, 8 Hz)	6.58 and 6.74 (1H each, dd, J = 2.0, 8.2 Hz)	6.96 (2H, m)
caff C2′,2″-H	7.00 (2H, d, J = 2 Hz)	6.81 and 6.92 (1H each, d, J = 2.0 Hz)	7.07 (2H, d, J = 1.6 Hz)
caff C7′,7″-H	7.49 (2H, d, J = 16 Hz)	7.46 and 7.48 (1H each, d, J = 15.9 Hz)	7.42 (1H, d, J = 16.0 Hz), 7.46 (1H, d, J = 16.0 Hz)

^{13}C NMR (CD_3OD, 100 MHz)

	C1	Cynarin[a]	Cynarin[b]
(C-2)	36.7 (t)	32.9 (t)	36.8 (t)
(C-6)	41.3 (t)	41.3 (t)	38.4 (t)
(C-5)	68.3 (d)	67.8 (d)	71.0 (d)
(C-3)	73.0 (d)	73.0 (d)	71.8 (d)
(C-4)	74.8 (d)	75.3 (d)	74.5 (d)
(C-1)	75.4 (s)	81.1 (s)	84.0 (s)
(caff C-2′,2″)	113.6 (d), 113.6 (d)	115.4, 115.5 (d)	115.0 (d), 115.0 (d)
(caff C-8′,8″)	114.0	115.1 (d)	115.4 (d), 115.0 (d),
(caff C-5′,5″)	115.0	116.1, 116.6 (d)	116.8 (d), 116.5 (d)
(caff C-6′,6″)	121.3	122.0, 123.0 (d)	123.0 (d), 122.8 (d)
(caff C-1′,1″)	126.3	127.4, 127.5 (s)	128.1 (s), 127.7 (s),
(caff C-7′,7″)	145.3	146.5, 146.7 (s)	146.7 (s), 146.2 (s),
(caff C-3′,3″)	145.5	147.2, 147.8 (d)	146.9 (d), 146.8 (d),
(caff C-4′,4″)	148.0	149.3, 149.7 (s)	149,7 (s), 149.3 (s)
(caff C-9′,9″)	169.5	167.8, 168.9 (s)	169.2 (s), 168.3 (s)
(−COOH)	178.3 (s)	174.6 (s)	178.2 (s)

[a] Reference 23. [b] Reference 24.

agents. In addition, specifically in this study, a novel immunosuppression in vitro was found for *Echinacea*, which has been purported to boost the immune system in humans. The full potential of AFTIR depends on its successful scaling-up with microchip (see Figure 13). Future studies could perhaps deploy AFTIR with "bait" receptors integral to cancer or inflammation, seeking anti-cancer and antiinflammatory agents.

Experimental Procedures

Receptors and Proteins. Human CD28-muIg and CD80-muIg fusion proteins were purchased from ID Labs Inc. CD28-muIg is a soluble fusion protein consisting of the extra-cellular (134 aa) domain of human CD28 fused to murine IgG2a Fc (233 aa). CD80-muIg is a soluble fusion protein consisting of the extra-cellular (173 aa) domain of human CD80 fused to murine IgG2a Fc (232 aa). Both were purified from the tissue culture supernatant of CHO transfectants by protein A and size exclusion chromatography. Anti-human CD28 antibody and anti-human CD3 antibody were purchased from BioLegend. In the experiments, the quantity of anti-CD28 and CD80 used was only around 2% the quantity of CD28 immobilized.

Chemicals and Reagents. Sensor chip CM5, HEPES buffer solution HBS-EP (10 mM HEPES, 0.15 M NaCl, 3.4 mM EDTA, 0.05% surfactant P20, pH 7.4), and amine-coupling kit (*N*-hydroxysuccinimide (NHS), *N*-ethyl-*N*′-(3-diethylaminopropyl) carbodiimide (EDS), and ethanolamine hydrochloride) were obtained from Biocore AB (Uppsala, Sweden). Solvent used for chromatographic analysis was ChromAB grade of MeOH (Mallinckrodt, code no. 3041-68, suitable for liquid chromatography). Trifluoroacetic acid (TFA; 99% purity, Fluka) was used for eluent pH adjustment. Water used in this study was deionized and distilled. The Cynarin reference standard was obtained from Fleton Reference Substance Co., Ltd. (Batch No. CHI20041218, 98.4%). FK-506 and ionomycin were purchased from CalBiochem, and both of them were dissolved by DMSO at a final concentration of 1 μg/mL. Phorbol 12-myristate 13-acetate (PMA) was purchased from Sigma. PMA was dissolved by DMSO and stored at −20 °C. MTT (3-[4,5-dimethylthiazol-2-yl]-2,5-diphenyltetrazolium bromide) was purchased from Sigma.

Preparations of CEE and Target Compounds. Fifty grams of *Echinacea* powder (*Echinacea purpurea*, SaveOn-Albertson's Inc.) was extracted with 100% dd-H_2O (1000 mL) by stirring at room temperature for 72 h. The water extracts were collected and filtered through filter paper (No.1, code no. PW300-1125, pore size = 10 μm, TOYO Inc.). Extraction was repeated three times. All filtrates were collected and concentrated to 500 mL under reduced pressure. Next, 4000 mL acetone was added to the concentrate, and the solution was stored at −20 °C for 24 h. Afterward, the solution was centrifuged at 8000 rpm for 60 min. The supernatant was collected and then completely dried under reduced pressure. The final crude extract of *Echinacea* (CEE) was then used for the AFTIR experiment. The target compounds C1−C5 were collected as stated in the Results (Figure 7).

Surface Plasmon Resonance Analysis. BIAcore 3000 (Biacore, Uppsala, Sweden) was employed for real-time biospecific interaction analysis. Binding analysis was performed at 25 °C with a flow rate of 10 μL/min. In general, proteins were immobilized on a layer of carboxylated dextran on a CM5 sensor chip (research grade; Biacore) by amine coupling.[26] Samples were diluted in HBS running buffer (10 mM HEPES, pH 7.4, 150 mM NaCl, 3.4 mM EDTA, 0.005% surfactant P20) to a final concentration of 15−30 μM before injection. Afterward, 50 mM NaOH buffer was posed through cell to remove bound material. Extracts were injected at different concentrations from 1.9 to 60 μM. The binding constant between immobilized receptor (imm-CD28) and ligand was determined using BIAevaluation 3.1 software (Biacore).

High Performance Liquid Chromatography (HPLC) Analysis. HPLC analysis was performed on an HP Technologies 1100 Series HPLC Modules with 250 × 4.6 mm Discovery BIO Wide Pore C18 HPLC column (SUEPLCO). The machine was connected

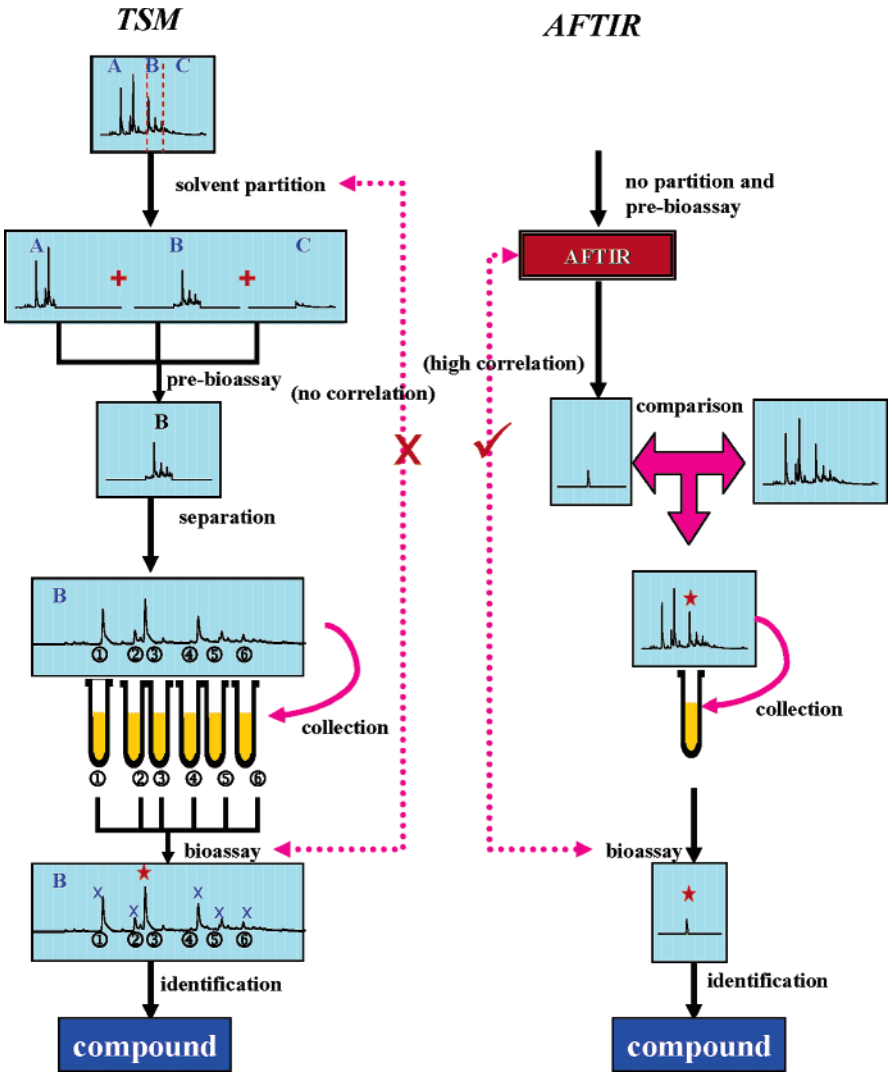

Figure 12. A schematic comparison of the traditional screening method (TSM) and after flowing through immobilized receptor (AFTIR). The greatest advantage of using AFTIR is to select a target molecule from herbs with the desired biological function. There was a high correlation to identify active compound(s) between the beginning of screening and the later bioassay. The isolation of a desired peak from HPLC after the treatment of AFTIR is a unique step in comparison to TSM.

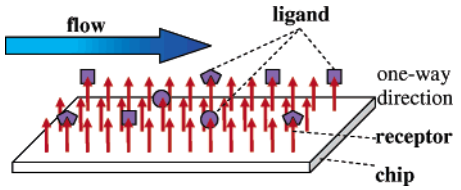

Figure 13. AFTIR miroarray setup. This investigation presents AFTIR with one immobilized receptor species. The future of AFTIR lies with micro-array concepts, simultaneously fluxing herbal extract across a large number of different chip-immobilized receptor species.

to a diode array detector. Two organic solvents were applied as eluents: eluent A (99.95% H_2O/0.05% TFA (v/v)) and eluent B (99.95% MeOH/0.05% TFA (v/v)). Both eluents were filtered under vacuum and then degassed. Injections of 20 μL of CEE into the column were chromatographed using the program provided by manufacturer (ChemStation, HP). The analysis of sample using solvent eluent was as follows: eluent A was injected first for 10 min and followed by a linear gradient from 0% to 100% of eluent B for over 60 min. Eluent B was continuously maintained for 10 min at a flow rate 0.6 mL/min. The compound(s) of CEE eluted from the column was monitored at $UV_{330\ nm}$. HPLC spectra were obtained and used for comparison before and after AFTIR experiments.

LC−MS Analysis. Atmospheric pressure ionization mass spectrometry analysis was performed on a Quattro LC benchtop triple quadrupole mass spectrometer (JASCO international, Japan). The machine was operated by electrospray ionization with a negative mode (ES^-) interface. Mass spectrometric data were acquired in the full scan mode in the range of *m*/*z* between 150 and 600. Sensitivity of the mass spectrometer was optimized using the Cynarin standard from Fleton Reference Substance Co., Ltd. Agilent 1100 HPLC system was used for the separation of samples and standards. The Luna C18(2) column and mobile phase gradient were identical to those used for RP-HPLC-UV analysis described above, and 5 μL of C1 samples was injected per run by manual injector. The flow rate was fixed at 0.12 mL/min. Spectrometric analysis was done using MassLynx 3.5 software (Micromass Ltd.).

NMR Spectroscopy. C1 compound isolated and collected by chromatography (see the section on collection of C1 compound above) was dissolved in 0.8 mL of CD_3OD. ^1H and ^{13}C NMR spectra were acquired at 25 °C by using a Bruker QE 400 MHz NMR spectrometer. Chemical shift values[25] were assigned relative to the frequencies of residual nondeuterated water and methanol externally referenced to tetramethylsilane. The chemical shifts of the ^1H NMR (CD_3OD) spectrum of C1 compound were obtained as follows: δ: 2.03−2.13 (2H, m) and 2.16−2.28 (2H, m, C2,6-H), 3.85 (1H, m, C3−H), 3.55 (1H, d, J = 4 Hz, C4−H), 3.15 (1H, dd, J = 3, 9 Hz, C5−H), 4.81 (4H, s, caff −OH), 6.18 (2H, d, J = 16 Hz, caff C8′,8″-H), 6.74 (2H, d, J = 8 Hz, caff C5′,5″-

H), 6.89 (2H, dd, $J = 2$, 8 Hz, caff C6′,6″-H), 7.00 (2H, d, $J = 2$ Hz, caff C2′,2″-H), 7.49 (2H, d, $J = 16$ Hz, caff C7′,7″-H). The chemical shifts of the ^{13}C NMR (CD_3OD) spectrum of C1 compound were as follows: δ: 36.7 (C-2), 41.3 (C-6), 68.3 (C-5), 73.0(C-3), 74.8 (C-4), 75.4 (C-1), 178.3 (−COOH), 113.6 (caff C-2′,2″), 114.0 (caff C-8′,8″), 115.0 (caff C-5′,5″), 121.3 (caff C-6′,6″), 126.3 (caff C-1′,1″), 145.3 (caff C-7′,7″), 145.5 (caff C-3′,3″), 148.0 (caff C-4′,4″), 169.5 (caff C-9′,9″). Based on mass spectroscopy and NMR assignments, the formula and structure of C1 compound was revealed as that shown in the Results; Figure 11.

Stimulation of T-cell. Jurkat leukemic T-cells were maintained in a humidified atmosphere of 5% CO_2/95% air at 37 °C in RPMI-1640 medium (HyClone, UT) including penicillin, streptomycin, and 10% heat-inactivated FBS. Two modes of T-cell stimulations were used for the present experiments: anti-CD3 plus anti-CD28 (CD28-dependent stimulation) and PMA plus ionomycin (CD28-independent stimulation). The detail pathways of these two modes are shown in Figure 8. For CD28-dependent stimulation experiment, flat-bottom 96-well plates were coated with 10 μg/mL of anti-CD3 for 24 h at 4 °C. Wells including anti-CD3 were then washed twice with PBS to remove unbound anti-CD3. Jurkat T-cells (200 μL, 2×10^6 cells/mL) with soluble anti-CD28 (1 μg/mL) were then added to the wells. The cells were activated by anti-CD3 already existing in the wells. During T-cell stimulation, the plate was incubated for 24 h at 37 °C. Cell solution (100 μL) was then tested for IL-2 by enzyme-linked immuno-sorbent assay (ELISA; kit was purchased from Biosource, CA). For the CD28-independent stimulation experiment, 200 μL of Jurkat cell (5×10^5 cells/mL) was incubated with PMA (50 nM)/ionomycin (1 μg/mL) for 24 h at 37 °C. 100 μL of cell solution was then tested for IL-2 by ELISA. For CEE and C1 experiments on T-cell, these materials were added into culture plates containing the cells and preincubated at 37 °C for 15 min before stimulation (either for CD28-dependent or for CD28-independent stimulation). The culture supernatants in both modes above were harvested after 24 h incubation at 37 °C. Details about IL-2 concentration measurement after T-cell activation are given below.

IL-2 ELISA Assay. A 96-well flat-bottom plate was coated with anti-IL-2 mAb (100 μL at 4 μg/mL) in phosphate-buffered saline (PBS; pH 7.3) at room temperature overnight. The plate was then washed with PBS containing 0.05% Tween 20 (PBS-T) three times. Subsequently, the plate was incubated with a blocking solution containing 1% bovine serum albumin in PBS for more than 1 h. 100 μL of cell solution and 50 μL biotinylated anti-IL-2 detection antibodies (12.5 ng/mL) were added to each well after being washed with PBS-T buffer, and they were incubated at room temperature for 2 h. Subsequently, 100 μL of streptavidin horseradish peroxidase (1/2000 dilution of a 1.25 mg/mL solution) was added after washing with PBS-T buffer again, and the solution was incubated for 30 min at room temperature. Washing the cell medium with PBS-T buffer again, 100 μL of substrate solution containing a 1/1 mixture of H_2O_2 and tetramethylbenzidine was added and the solution was incubated for 25 min at room temperature. The reaction was terminated by the addition of 100 μL of stop solution (1 M H_2SO_4). The concentration of IL-2 was then measured with a microplate reader. The amount of IL-2 was calculated as the relative percentage to 1200 pg/μL (i.e., 1200 pg/μL of IL-2 was defined as 100%). One-way ANOVA (superANOVA statistical software, Berkeley, CA) was used for both measurements of IL-2 production and cytotoxicity in T-cells induced by FK-506, CEE, and C1 within a P value smaller than 0.05.

MTT Colorimetric Assay. Cytotoxicity of T-cells during the CEE or C1 stimulation was measured by MTT (3-[4-dimethylthiazol-2-yl]-2,5-diphenyl-tetrazolium bromide) colorimetric assay. 100 μL of Jurkat cells (5×10^5 cells/mL) was incubated for 24 h at 37 °C with various concentrations of CEE and C1. The cell solution was then centrifuged at 200g for 10 min, and its supernatant was removed. 25 μL of MTT (5 mg/mL in H_2O) was added, and the cell solution was again incubated at 37 °C for 4 h. Afterward, 200 μL of lysis buffer (DMSO) was added, and the concentration of dissolved MTT crystals was measured with an ELISA reader (Dynatech, Chantilly, VA). The survival rate (%) was determined as $OD_{560\,nm}$ of test sample (CEE or C1)/$OD_{560\,nm}$ of control (PBS buffer only) × 100%.

Acknowledgment. We thank Prof. Kan, Lou-Sing at Institute of Chemistry, Academia Sinica, for help with the BIACORE 3000. This work was supported by a grant from the National Science Council of Taiwan (NSC91-3112-P-001-035-Y).

References

(1) Normile, D. Asian medicine. The new face of traditional Chinese medicine. *Science* **2003**, *299*, 188−90.
(2) Basu, P. Trading on traditional medicines. *Nat. Biotechnol.* **2004**, *22*, 263−5.
(3) Bent, S.; Ko, R. Commonly used herbal medicines in the United States: a review. *Am. J. Med.* **2004**, *116*, 478−85.
(4) Chan, K. Chinese medicinal materials and their interface with Western medical concepts. *J. Ethnopharmacol.* **2005**, *96*, 1−18.
(5) Cai, Z.; Lee, F. S.; Wang, X. R.; Yu, W. J. A capsule review of recent studies on the application of mass spectrometry in the analysis of Chinese medicinal herbs. *J. Mass Spectrom.* **2002**, *37*, 1013−24.
(6) Mao, X.; Kong, L.; Luo, Q.; Li, X.; Zou, H. Screening and analysis of permeable compounds in Radix Angelica Sinensis with immobilized liposome chromatography. *J. Chromatogr., B* **2002**, *779*, 331−9.
(7) Taylor, J. A.; Weber, W.; Standish, L.; Quinn, H.; Goesling, J.; McGann, M.; Calabrese, C. Efficacy and safety of echinacea in treating upper respiratory tract infections in children: a randomized controlled trial. *JAMA, J. Am. Med. Assoc.* **2003**, *290*, 2824−30.
(8) Barrett, B. P.; Brown, R. L.; Locken, K.; Maberry, R.; Bobula, J. A.; D'Alessio, D. Treatment of the common cold with unrefined echinacea. A randomized, double-blind, placebo-controlled trial. *Ann. Intern. Med.* **2002**, *137*, 939−46.
(9) Melchart, D.; Linde, K.; Worku, F.; Sarkady, L.; Holzmann, M.; Jurcic, K.; Wagner, H. Results of five randomized studies on the immunomodulatory activity of preparations of Echinacea. *J. Altern. Complement Med.* **1995**, *1*, 145−60.
(10) Breittmayer, J. P.; Bernard, A.; Aussel, C. Regulation by sphingomyelinase and sphingosine of Ca2+ signals elicited by CD3 monoclonal antibody, thapsigargin, or ionomycin in the Jurkat T cell line. *J. Biol. Chem.* **1994**, *269*, 5054−8.
(11) Chatila, T.; Silverman, L.; Miller, R.; Geha, R. Mechanisms of T cell activation by the calcium ionophore ionomycin. *J. Immunol.* **1989**, *143*, 1283−9.
(12) Darrow, T. L.; Quinn-Allen, M. A.; Crowley, N. J.; Seigler, H. F. Modulation of in vitro autologous melanoma-specific cytotoxic T-cell responses by phorbol dibutyrate and ionomycin. *Cell. Immunol.* **1990**, *125*, 508−17.
(13) Dupuis, G.; Bastin, B. Lectin interactions with the Jurkat leukemic T-cell line: quantitative binding studies and interleukin-2 production. *J. Leukocyte Biol.* **1988**, *43*, 238−47.
(14) Bubenik, J.; Indrova, M.; Simova, J.; Kypenova, H.; Bubenikova, D.; Dolezalova, K. Phorbol myristate acetate-stimulated production of interleukin 2 by T-cell lymphoma and constitutive production by derived hybridomas. *Neoplasma* **1984**, *31*, 497−505.
(15) Mukaida, N.; Kasahara, T.; Shioiri-Nakano, K.; Kawai, T. Interleukin 2-dependent T cell line acquires responsiveness to phorbol myristate acetate and lipopolysaccharide in the course of long-term culture. *Immunol. Commun.* **1984**, *13*, 475−86.
(16) Stimpel, M.; Proksch, A.; Wagner, H.; Lohmann-Matthes, M. L. Macrophage activation and induction of macrophage cytotoxicity by purified polysaccharide fractions from the plant Echinacea purpurea. *Infect. Immun.* **1984**, *46*, 845−9.
(17) Northoff, H.; Stoeck, M.; Krammer, P. H. The effect of phorbol-myristate acetate and concanavalin A on the growth of interleukin-2-dependent T-cell lines. *Immunobiology* **1982**, *161*, 464−75.
(18) Li, L.; Yee, C.; Beavo, J. A. CD3- and CD28-dependent induction of PDE7 required for T cell activation. *Science* **1999**, *283*, 848−51.
(19) Hutchcroft, J. E.; Slavik, J. M.; Lin, H.; Watanabe, T.; Bierer, B. E. Uncoupling activation-dependent HS1 phosphorylation from nuclear factor of activated T cells transcriptional activation in Jurkat T cells: differential signaling through CD3 and the costimulatory receptors CD2 and CD28. *J. Immunol.* **1998**, *161*, 4506−12.
(20) Nijhuis, E. W.; vd Wiel-van Kemenade, E.; Figdor, C. G.; van Lier, R. A. Activation and expansion of tumour-infiltrating lymphocytes by anti-CD3 and anti-CD28 monoclonal antibodies. *Cancer Immunol. Immunother.* **1990**, *32*, 245−50.

(21) Baroja, M. L.; Lorre, K.; Van Vaeck, F.; Ceuppens, J. L. The anti-T cell monoclonal antibody 9.3 (anti-CD28) provides a helper signal and bypasses the need for accessory cells in T cell activation with immobilized anti-CD3 and mitogens. *Cell. Immunol.* **1989**, *120*, 205−17.

(22) Bjorndahl, J. M.; Sung, S. S.; Hansen, J. A.; Fu, S. M. Human T cell activation: differential response to anti-CD28 as compared to anti-CD3 monoclonal antibodies. *Eur. J. Immunol.* **1989**, *19*, 881−7.

(23) Zhu, X.; Zhang, H.; Lo, R. Phenolic compounds from the leaf extract of artichoke (Cynara scolymus L.) and their antimicrobial activities. *J. Agric. Food Chem.* **2004**, *52*, 7272−8.

(24) Wang, M.; Simon, J. E.; Aviles, I. F.; He, K.; Zheng, Q. Y.; Tadmor, Y. Analysis of antioxidative phenolic compounds in artichoke (Cynara scolymus L.). *J. Agric. Food Chem.* **2003**, *51*, 601−8.

(25) Tolonen, A.; Joutsamo, T.; Mattlla, S.; Kamarainen, T.; Jalonen, J. Identification of isomeric dicaffeoylquinic acids from Eleutherococcus senticosus using HPLC-ESI/TOF/MS and 1H NMR methods. *Phytochem. Anal.* **2002**, *13*, 316−28.

(26) Johnsson, B.; Lofas, S.; Lindquist, G. Immobilization of proteins to a carboxymethyldextran-modified gold surface for biospecific interaction analysis in surface plasmon resonance sensors. *Anal. Biochem.* **1991**, *198*, 268−77.

JM0509039